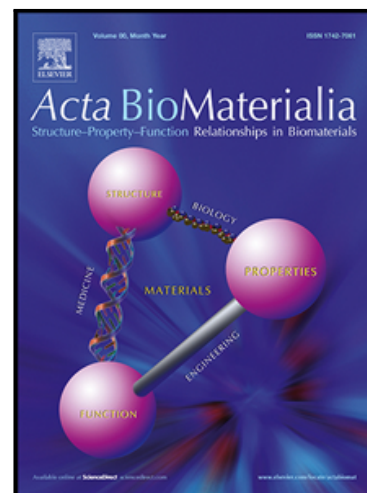# Journal Pre-proof

Engineered aligned endothelial cell structures in tethered collagen hydrogels promote peripheral nerve regeneration

Papon Muangsanit , Victoria Roberton , Eleni Costa ,
James Phillips

Please cite this article as: Papon Muangsanit , Victoria Roberton , Eleni Costa , James Phillips , Engineered aligned endothelial cell structures in tethered collagen hydrogels promote peripheral nerve regeneration, *Acta Biomaterialia* (2021), doi: https://doi.org/10.1016/j.actbio.2021.03.039

Engineered aligned endothelial cell structures in tethered collagen hydrogels promote peripheral nerve regeneration

Papon Muangsanit [a,b,c, *], Victoria Roberton [b,c], Eleni Costa [c], James Phillips [a,b,c]

[a]Department of Biomaterials and Tissue Engineering, Eastman Dental Institute, University College London, 256 Grays Inn Rd, London WC1X 8LD, United Kingdom

[b]UCL Centre for Nerve Engineering, University College London, London, United Kingdom

[c]Department of Pharmacology, UCL School of Pharmacy, University College London, 29-39 Brunswick Square, Bloomsbury, London WC1N 1AX, United Kingdom

*Corresponding Author.
Papon Muangsanit
Department of Pharmacology, UCL School of Pharmacy, University College London, 29-39 Brunswick Square, Bloomsbury, London WC1N 1AX, United Kingdom
Email: papon.muangsanit.14@ucl.ac.uk

Statement of Significance

Nerve tissue engineering provides a potential way to overcome the limitations associated with current clinical grafting techniques for the repair of severe peripheral nerve injuries. However, the therapeutic cells within engineered nerve tissue require effective vascularisation in order to survive. This work therefore aimed to develop engineered nerve constructs containing aligned tube-like structures made from endothelial cells. Not only did this provide a method to improve vascularisation, it demonstrated for the first time that aligned endothelial cells can outperform Schwann cells in promoting nerve regeneration in the rat sciatic nerve model. This has introduced the concept of developing pre-vascularised engineered nerve tissues, and indicated the potential usefulness of endothelial cell structures in tissue engineering for peripheral nerve repair.

Abstract

Vascularisation is important in nerve tissue engineering to provide blood supply and nutrients for long-term survival of implanted cells. Furthermore, blood vessels in regenerating nerves have been shown to serve as tracks for Schwann cells to migrate along and thus form Bands of Büngner which promote axonal regeneration. In this study, we have developed tissue-engineered constructs containing aligned endothelial cells, or co-cultures of both endothelial cells and Schwann cells to test whether these structures could promote regeneration across peripheral nerve gaps. Type I rat tail collagen gels containing HUVECs (Human Umbilical Vein Endothelial Cells, 4×10^6 cells/ml) were cast in perforated tethering silicone tubes to facilitate cellular self-alignment and tube formation for 4 days of culture. For co-culture constructs, optimal tube formation and cellular alignment was achieved with a ratio of $4:0.5\times10^6$ cells/ml (HUVECs:Schwann cells). An *in vivo* test of the engineered constructs to bridge a 10 mm gap in rat sciatic nerves for 4 weeks revealed that constructs containing only HUVECs significantly promoted axonal regeneration and vascularisation across the gap, as compared to conventional aligned Schwann cell constructs and those containing co-cultured HUVECs and Schwann cells. Our results suggest that tissue-engineered constructs containing aligned endothelial cells within collagen matrix could be good candidates to treat peripheral nerve injury.

1   Introduction

Vascularisation is essential for tissue-engineered constructs in terms of support for cell survival after implantation and overall healing efficacy *in vivo* [1]. The ingrowth of blood vessels from the host to the implanted tissue construct often takes time, resulting in limited nutrients, hypoxic conditions and potential necrosis of the implant [2]. To date, several studies have aimed to develop vascularised tissue-engineered constructs to improve the efficacy of tissue regeneration [3-5], however studies focussed on the optimisation of vascularisation in peripheral nerve tissue engineering are lacking.

In the peripheral nervous system, in addition to providing perfusion, blood vessels can act as guidance cues for Schwann cell migration and neuronal regeneration [6-9]. Endothelial cells, which mainly constitute the inner lining of blood vessels, are known to synthesise several factors that are supportive of nerve regeneration. When subventricular zone explants from the adult rat brain are co-cultured with endothelial cells, neurite outgrowth and migration of neurons are enhanced [9]. Similarly, vitronectin and heparin sulphate proteoglycans, glycoproteins expressed on the surface of endothelial cells, are involved in neurite activity and growth [10]. A study by Jauhiainen *et al.* (2019) showed that fibronectin and leucine-rich

transmembrane protein-3 (FLRT3), an axon guidance-related factor, regulates both VEGF-signalling and endothelial cell functions [11]. Furthermore, Grasman and Kaplan (2017) reported that human umbilical cord vein endothelial cells (HUVECs) enhanced axonal growth from rat dorsal root ganglia by secreting neurotrophic factors, specifically brain-derived neurotrophic factor (BDNF), and growing axons were found to be in close proximity to clusters of HUVECs [8]. The surface of the blood vessel itself has also been demonstrated to support Schwann cell migration and formation of the bands of Büngner that help axonal regeneration following nerve injury [7].

The intrinsic vasculature of the nerves predominantly exhibits a longitudinally oriented pattern, which is anastomosed to the adjacent vasa nervorum, suggesting the relevance of incorporating aligned micro-vessels in nerve engineered substitutes. Although some vascularised nerve grafting approaches have been used in the clinic, the use of donor nerve that can remain attached to vascular pedicles is the primary selection criteria for such grafts, which involves limited availability and leads to donor site morbidity [12-15]. As a result, pre-vascularised tissue-engineered nerve constructs provide a useful new opportunity for investigation.

Several approaches to enhance the vascularisation of tissue-engineered constructs have been developed, such as incorporating angiogenic growth factors [16, 17] or using genetically modified cells that over-express angiogenic genes [18, 19]. However, these approaches promote vascularisation by driving the angiogenic response in the surrounding host tissue, which may not vascularise larger grafts rapidly enough to support engrafted cell survival. A variety of approaches to generate engineered micro-vessels *in vitro* have been investigated. For example, mouse aortic endothelial cells seeded in a mixture of collagen gel and fibronectin, embedded in polydimethylsiloxane (PDMS) microchannels, formed vessels *in vitro* under laminar shear stress from fluid flow [20]. Other investigators have successfully developed blood vessels using endothelial cells embedded in fibrin-coated dextran microbeads or endothelial cell spheroids entrapped in fibrin gels and shown the ability to orient these vessels by applying tensional forces or magnetic fields [21, 22]. Some researchers also employed an intrinsic capability of endothelial cells to self-assemble into a network of micro-vessels within an ECM scaffold [23-26]. For example, HUVECs co-cultured with fibroblasts in collagen scaffolds supplemented with chitosan and glycosaminoglycan promoted the spontaneous formation of capillary networks [24]. Other studies showed that self-aligned tethered co-cultures of HUVECs and pericytes in fibrin gels formed highly interconnected microvascular patches for use as a component in cardiac tissue engineering [27, 28].

For nerve tissue engineering, aligned cellular scaffolds have been developed to mimic the supportive anisotropic Schwann cell environment present within nerve autografts, which are the current preferred clinical option for repairing severe nerve damage. Aligned Schwann cell-populated collagen gels tethered within silicone tubes undergo cellular self-alignment to form an anisotropic guidance substrate to support and guide neuronal regeneration [29]. Subsequent translational research has developed this concept further, incorporating stem cell-derived therapeutic cells, additional stabilisation steps, and bioresorbable outer tube materials [30-32]. However, implantation of dense cellular conduits can lead to challenges associated with local hypoxia and ischaemia, potentially causing the engrafted cells to adopt a phenotype that prioritises angiogenesis over regeneration support [33], or resulting in cell death and wastage of valuable therapeutic cells. Incorporating pre-engineered vascular structures may therefore offer a suitable approach to improve perfusion and overcome the problem of necrosis in tissue-engineered cellular nerve grafts, while simultaneously providing an additional directional growth substrate to support and guide neuronal regeneration [7].

The aim of this study was to develop aligned vascular structures using endothelial cells in tethered collagen hydrogels as a new approach for nerve tissue engineering. The addition of Schwann cells to the aligned endothelial cell structures was also investigated, yielding constructs containing both aligned tube-like endothelial cell structures and Schwann cells, which mimics key cellular components and architecture of native nerve tissue. The ability of these constructs to support and guide neuronal regeneration and vascularisation *in vivo* was investigated using a rat sciatic nerve injury model.

2   Method

2.1   Cell culture

Human umbilical vein endothelial cells (HUVECs; PromoCell) were grown in complete Endothelial Cell Growth Media (EGM) (PromoCell). They were used between passages 4 and 10. Schwann cells were from the rat Schwann cell line SCL4.1/F7 (Health Protection Agency) and were grown in culture medium (Dulbecco's Modified Eagle's Medium, DMEM; Gibco). They were used between passages 4 and 20. All media were supplemented with 10% v/v heat-inactivated foetal bovine serum (FBS; Thermo Fisher Scientific) and 1% v/v Penicillin/Streptomycin (Gibco) and replaced every 2 days. All cell cultures and subsequent experiments were maintained in a humidified incubator with 5% CO_2/95% air at 37 ºC.

2.2   Tissue engineering

2.2.1   *Creation of tethering holes in silicone tubes*

Medical-grade silicone tubes (inner diameter, 1.98 mm and outer diameter, 3.17 mm; Syndev) were cut to be 12 mm in length. Two rings of eight square holes (approximately 0.9 mm sides) around each end of the silicone tube (16-hole construct, figure 1) were made with a 19-gauge hypodermic needle under a dissection microscope. The holes allowed the collagen gels that were subsequently formed within the tubes to become tethered exclusively at the ends of the tubes during contraction [29].
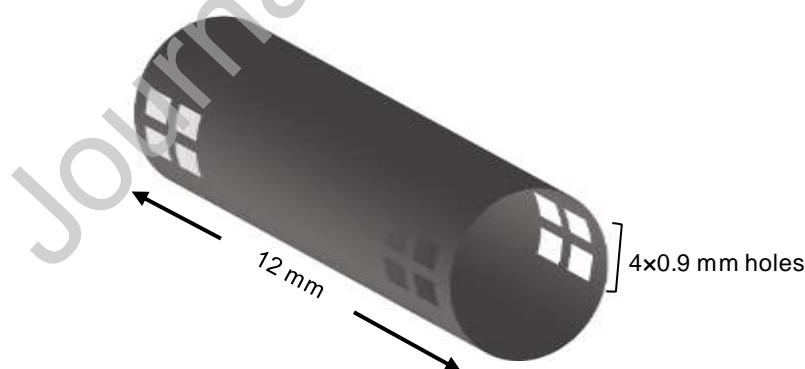
Figure 1. Schematic diagram showing the tethering holes in the walls of each end of the silicone tube.

2.2.2   *Fabrication of collagen gels*

To prepare 1 ml of collagen gel, 100 µl of 10× minimum essential medium (Sigma-Aldrich) was mixed with 800 µl of type 1 rat tail collagen (2 mg/ml in 0.6% acetic acid; FirstLink) and the mixture was neutralised using 43 µl of sodium hydroxide (diluted 1:10 in phosphate-buffered saline, PBS; Gibco) before an addition of 100 µl of cell suspension (culture medium

6

containing 0.5-4.0×10^6 cells/ml as required). For multi-well plate assays, 75 µl of the mixture was added to individual wells of 96-well plates. For aligned gels, the engineered neural tissue (EngNT) system was used according to methods described previously [34]. Briefly, 400 µl of the collagen and cell mixture was added to each rectangular EngNT mould at 4 °C and incubated at 37 °C for 15 min to allow gels to set. Cellular gels were then immersed in culture medium and incubated at 37 °C in a humidified chamber with 5% CO_2/95% air for at least 24 h to allow alignment to develop. This cellular self-alignment process has been characterised in detail previously and involves simultaneous organisation of cells and collagen fibrils [35]. Aligned cellular gels were then stabilised via plastic compression using RAFT absorbers (Lonza, Germany) for further use *in vivo*. For fully-hydrated gels in perforated silicone tubes, 100 µl of cellular collagen gel was made. To ensure cells were evenly distributed within the hydrogel, cells were resuspended in the 100 µl of neutralised collagen solution by slowly mixing with a pipette (10 cycles were sufficient to distribute cells) before injecting 50 µl into the silicone conduit from one end using the pipette. The remaining 50 µl was used to fill and bridge between each tethering hole from the outside, then gels were incubated at 37°C for 15 min to set. Following gel setting, constructs were cultured for 1-4 days depending on the experiment. Contraction of the tethered gels resulted in an aligned cellular hydrogel of length 10 mm forming between the attachment points, leaving a 1 mm space at each end of the 12 mm silicone tubes to accommodate insertion of the nerve stumps. Final constructs for the *in vivo* tests were kept in cold Hibernate-A medium until surgical implantation.

2.3 Surgical repair of rat sciatic nerve

All surgical procedures were performed in accordance with the UK Animals (Scientific Procedures) Act (1986) / European Directive (2010/63/EU) and approved by the UCL Animal Welfare and Ethics Review Board. Eighteen wildtype male Wistar rats (225-300g) were randomised to three groups: Schwann cell (n=6), HUVEC (n=6), and Schwann cell-HUVEC combined (n=6). All the rats were given daily injections of the immunosuppressant cyclosporine A (Sandimmune, Novartis at 10 mg/kg body weight i.p., diluted in saline solution), to prevent immune response to the transplanted cells. Dosing began three days prior to surgery and was continued daily for the duration of the experiment. Rats were deeply anesthetised by inhalation of 5% isoflurane in O_2 in an induction chamber, and anaesthesia maintained with 2-2.5% isoflurane delivered via a mask throughout surgery. The left sciatic nerve was exposed at mid-thigh level and transected to create a 10 mm gap. In all groups the conduit was implanted by insertion of the proximal and distal nerve stumps 1 mm into the 12 mm tube and coaptation to the conduit by two epineurial sutures (Ethilon 10/0; Ethicon-

Johnson & Johnson, Brussels, Belgium) at each stump. Wounds were then closed in layers and animals were allowed to recover for 4 weeks.

2.4 Preparation of nerves for histological analysis

At the end point, rats were culled using CO_2 asphyxiation and repaired nerves were excised and fixed in 4% paraformaldehyde (Sigma-Aldrich) for 24 h at 4 ºC. Fixed nerves were washed thoroughly with PBS and the silicone tube was removed and discarded. Nerves were incubated in 15% sucrose in PBS for ~30 min until tissues became submerged and then transferred to 30% sucrose in PBS overnight at 4 ºC. Nerve samples were then dissected into pieces for further analysis as shown in Figure 2. The segments were incubated for 2-4 h in 1:1 v/v 30% sucrose in PBS: optimal cutting temperature (OCT; Leica) solution. Samples were embedded in that 1:1 mixture in a cryosection mould (TAAB) and snap frozen in liquid nitrogen before storage at -80 ºC.
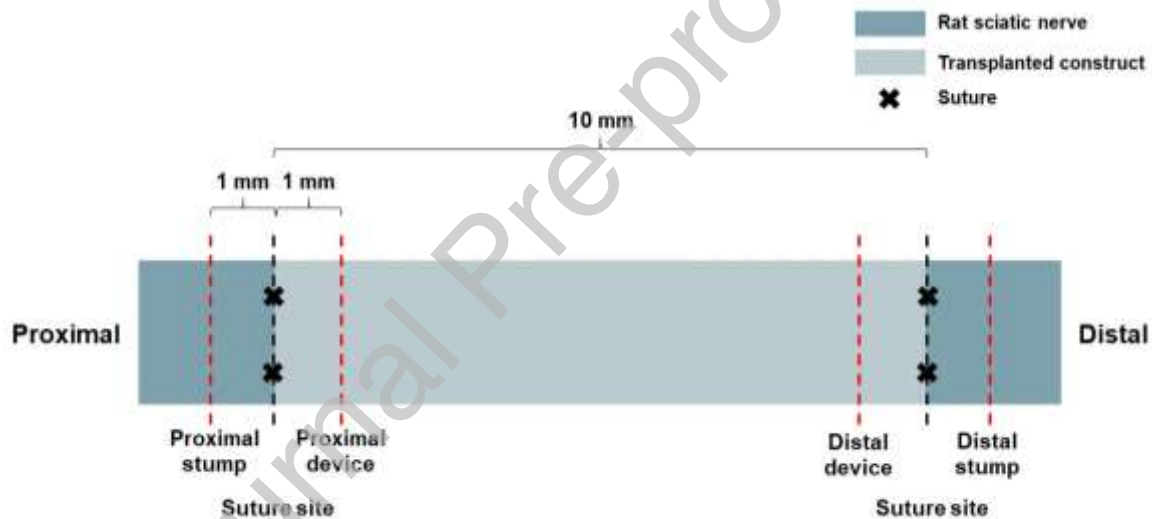

Figure 2. Schematic diagram of the nerve tissue preparation for histological analysis. Red dotted lines indicate the locations of the transverse sections.

Transverse sections (15 μm thick) were prepared from the proximal and distal stumps, at defined distances into the nerve stumps from the injury site, using a cryostat (Leica CM1860). The sections were adhered to glass slides (Superfrost TM Plus, Thermo Fisher Scientific) for histological analysis. The transverse sections that were used for analysis were from positions 1 mm into the proximal and distal stumps, or 1 mm into the proximal and distal parts of the repair site, measured from the repair boundaries (suture sites) in each case (Figure 2).

2.5 Fluorescence labelling

8

For immunofluorescent staining, nerve sections were washed in PBS three times for 5 min each wash. They were then permeabilised using 0.3% Triton X-100 (Sigma-Aldrich) for 30 min, blocked using 10% goat serum (Sigma-Aldrich) for 1 h, and then incubated in primary antibodies (Table 1) overnight at 4 °C. All primary antibodies reacted with rat tissue with the exception of CD31 (DAKO), the mouse monoclonal antibody JC/70A which specifically detects human endothelial cells, providing a method to identify transplanted HUVECs within rat tissues. All antibody dilutions were performed in PBS with 10 % goat serum. The following day, tissue sections were washed three times for 5 min in PBS then incubated with appropriate DyLight-conjugated secondary antibodies at room temperature for at least 1 h. Finally, sections were washed three times with PBS for 5 min each wash and mounted using VECTASHIELD Hard-set Mounting Medium with DAPI (Vector Laboratories). For Isolectin GS-IB4 staining, the same protocol was used, with nerve sections incubated in the fluorescent conjugated Isolectin (1:50) for at least 1h, followed by washing and mounting as for immunofluorescence.

Cellular hydrogels from *in vitro* studies were fixed in 4% paraformaldehyde in PBS for 24 h at 4 °C, washed twice for 10 min with PBS, and then permeabilised in 5% Triton X-100 for 30 min at room temperature. Gels were then washed three times with PBS for 10 min each followed by incubating with 5% goat serum for 30 min at room temperature to block non-specific binding. Primary antibody (Table 1) was diluted in PBS and gels were incubated overnight at 4 °C. The following day the gels were washed six times for 5 min each wash in PBS and incubated with secondary antibody in PBS (1:250) for 90 min at room temperature then washed again with PBS. Finally, gels were stained with Hoechst 33258 (1:1000) for 5 min at room temperature and washed once more with PBS for 5 min.

For phalloidin staining, cellular hydrogels were permeabilised in 5% Triton X-100 for 30 min at room temperature. Gels were then washed three times with PBS for 10 min each followed by incubation with phalloidin diluted 1:40 in PBS for 30 min at room temperature. Gels were washed three times with PBS for 10 min each. Finally, gels were stained with Hoechst 33258 for 5 min at room temperature and washed once more with PBS for 5 min.

Table 1. Antibody/isolectin/phalloidin manufacturers, dilutions and incubation times.

Fluorescence labelling reagents				
Name	**Target species**	**Brand**	**Product code**	**Dilution**

CD31	Human	Dako	JC70A	1:200
S-100	Rat	Dako	Z0311	1:400
Neurofilament	Rat	Eurogentec	SMI-35-050	1:1000
Phalloidin	-	Thermo Fisher Scientific	A12379	1:40
Isolectin GS-IB4	Rat	Thermo Fisher Scientific	I32450	1:50
DyLight 549 anti-mouse IgG	Mouse	Vector Laboratories	DI-2549	1:250
DyLight 488 anti-rabbit IgG	Rabbit	Vector Laboratories	DI-1488	1:250

2.6 Microscopy and image analysis

Confocal micrographs of fluorescently labelled cells were captured using Zeiss LSM 710 confocal microscopy at 20x magnification. Laser power and wavelength intensity settings were kept consistent and fields were selected using a standardised sampling protocol. For each cellular gel, three z-stacks were acquired in the side regions and middle regions, each containing 20-30 images (depending on the intensity of the signal at various depths). The emission signals of Alexa Fluor-488, Alexa Fluor-549, Alexa Fluor- 647 and DAPI were assigned to the green, red, magenta and blue channels respectively. Images were then exported using Zeiss LSM Image Browser software.

Micrographs of cellular collagen hydrogels within the perforated silicone tubes were captured using a digital transmitted light inverted microscope (Invitrogen™ EVOS™ XL Core Imaging System). Image Composite Editor (Microsoft) was used to stitch overlapping images to generate a full view of the construct. For contraction analysis, gels were imaged after setting (0 h) and at 24 h and ImageJ software was used to determine the percentage change in area [36].

The degree of tube-like structure formation was measured using the Angiogenesis Analyser in ImageJ Software. For each gel, three maximum intensity z-stack confocal projections from both the middle and the side were reversed to 8-bit black and white for best recognition of individual structures by the Angiogenesis Analyser. The projections were cropped to remove regions where cobblestone layers were prominent, to prevent the software falsely recognising these as angiogenic structures. The mean tube length and orientation of tube-

like structures were quantified using Volocity™ software (Perkin Elmer, Waltham, MA) running automated 3D image analysis protocols.

For the analysis of axon growth *in vivo*, high contrast tile-scan confocal micrographs were used to quantify all the neurofilament positive axons present in each section. Counting was performed via Volocity™ software. The protocol settings remained consistent for each confocal micrograph. For each location within each nerve sample, three tissue sections were analysed. For the analysis of blood vessels *in vivo*, ImageJ software was used to count and measure the diameter of blood vessels in sections (three tissue sections measured per condition from 6 separate animals). For Schwann cell area measurement, the reconstructed confocal micrographs were converted to 8-bit greyscale using ImageJ software, the area corresponding to the nerve bridge or fibre was then selected, thresholded and made binary. The create selection function was used to automatically outline the thresholded area and then the stained area was quantified using the measurement function.

2.7   Statistical analysis

Statistical analyses of data were performed using GraphPad Prism 8.0.1. Prior to the statistical test, a Shapiro-Wilk normality test was used to determine whether repeats have a Gaussian distribution. For comparisons of experiments with two parameters a Student's T-test was performed for statistical significance and the standard error (SEM) was calculated for all. For experiments with multiple treatments for comparison, a one-way ANOVA statistical assessment (or Kruskal-Wallis test for non-parametric distribution) or a two-way ANOVA test was performed, accompanied by multiple comparison tests. Data showed in all graphs represent mean ± SEM, unless otherwise stated. Differences were considered significant when $p < 0.05$.

3   Results

3.1   HUVECs form aligned tube-like structures in tethered collagen gels

Self-alignment of cells in tethered collagen gels requires sufficient tension from the interaction between cells and matrix, which can be investigated by assessing the contraction of free-floating cellular gels. Determining the cell seeding density and culture time that achieves a certain threshold percentage contraction in free-floating gels (contraction profile), predicts the parameters likely to produce alignment throughout tethered gels [37]. Figure 3a shows the results of a 96-well plate assay used to quantify the contraction profile of HUVECs over a range of four cell densities: 0.5, 1, 2 and 4×10^6 cells/ml of collagen. Contraction increased with greater cell density, with almost 60% contraction achieved from 4×10^6 cells/ml (Figure 3b). It has been suggested that a cell seeding density that provides between 50-80% contraction produces highly aligned cells in tethered gels [37]. Therefore 4×10^6 cells/ml of collagen was used in the construction of tethered gels because this was the minimum density sufficient for alignment. Higher cell densities may have increased contraction further, but would increase the risk of over-contraction and detachment in tethered gels. Representative images of Phalloidin stained HUVECs within the gels and quantification of the network characteristics after 2, 4 and 8 days in culture are shown in Figure 3c-3h. The majority of cells within the gels were highly aligned at all time points, with the 4-day period showing the greatest alignment (Figure 3d). Tube-like structures were detected after 4 days of culture, whereas at day 2 the majority of cells had elongated individually but not formed structures, exhibiting a significantly lower number of meshes, branches, junctions and lengths Figure 3e-3h). After 8 days of culture, tube-like structures were not significantly improved in terms of average length and alignment when compared to 4 days in culture, therefore a 4-day culture period was established as the optimum culture time to achieve tube-like structures.
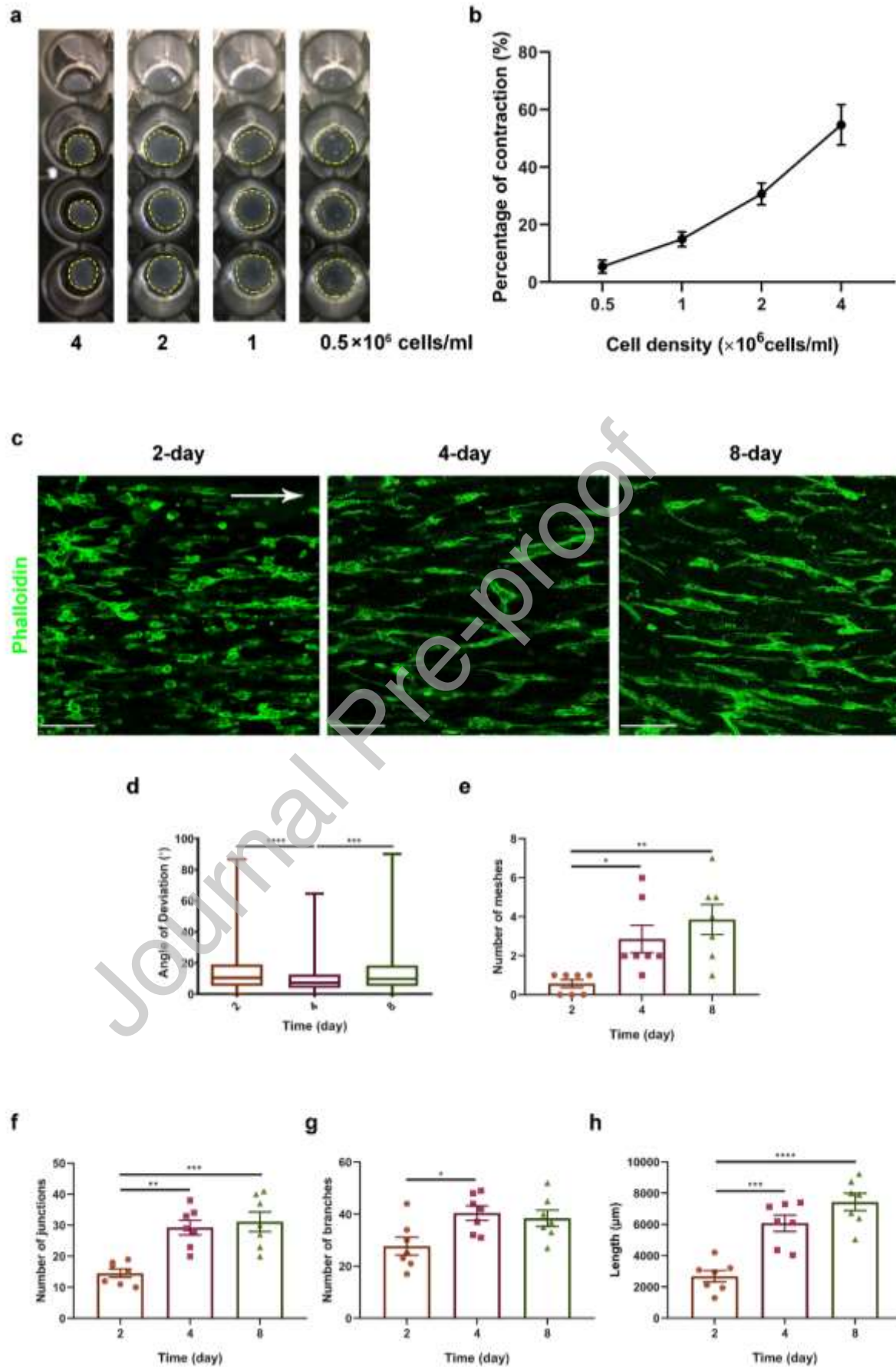
Figure 3. HUVECs formed highly aligned tube-like structures in tethered collagen gels using rectangular EngNT moulds. Free-floating collagen gels containing HUVECs at different seeding densities after 24 h in culture (dotted yellow line indicates the area of the top surface of the hydrogel after contraction) (**a**), enabled construction of a contraction profile (**b**), mean ± SEM, n=4 gels per condition from a total of three experimental gel batches. Percentage contraction was calculated by comparing the area of the top surface of each gel to the area of the well. The photographs were from slightly different angles of the same 96-well plate to accurately show the size of the contracted gels. (**c**) Confocal micrographs show aligned HUVECs and vascular networks following 3 culture periods: 2, 4 and 8 days, z-distance 20 μm, step size 1 μm. White arrow indicates the longitudinal axis of the tethered gels. Scale bars, 120 μm. (**d**) 3D image analysis was used to calculate the angle of deviation between HUVEC tube-like structure alignment and the longitudinal axis of the gel. Boxes show interquartile range and median values; whiskers indicate maximum and minimum angles (n=270 cells from 3 different experimental gel batches). The Kruskal-Wallis test was used to compute statistical significance for data in the box and whisker plot. Number of meshes (**e**), junctions (**f**), branches (**g**) and total branching length (**h**) were compared in 2-day, 4-day and 8-day cultured gels. Graphs show mean value ± SEM. n=7 gels. ****$P<0.0001$, ***$P<0.001$, **$P<0.01$, *$P<0.05$, one-way ANOVA with Dunn's multiple comparisons test was used for data in the bar graphs.

Having established the ability of HUVECs to form aligned tube-like structures in tethered collagen gels, the formation of such structures in co-culture with Schwann cells was investigated. To optimise the ratio between Schwann cells and HUVECs, engineered tissues were made with four different Schwann cell seeding densities while the number of HUVECs remained constant at 4×10^6 cells/ml gel. It was observed that a HUVEC:Schwann cell ratio of 4:0.5 showed significantly greater endothelial cell network formation compared with the other 3 ratios (Figure 4). Although there was no significant difference in the endothelial network formation in the 4:1 group compared to 4:0.5, the number of meshes (Figure 4d), junctions (Figure 4e), branches (Figure 4f), and total branching length (Figure 4g) of the 4:0.5 group were greater overall than in the other groups. In all cases, tube-like structures and Schwann cells were aligned with the longitudinal axis of the gels. From this experiment, the 4×10^6:0.5×10^6 ratio of HUVECs to Schwann cells was selected as the optimal co-culture seeding condition to yield both organised endothelial cell structures and aligned Schwann cells within a tethered collagen gel.
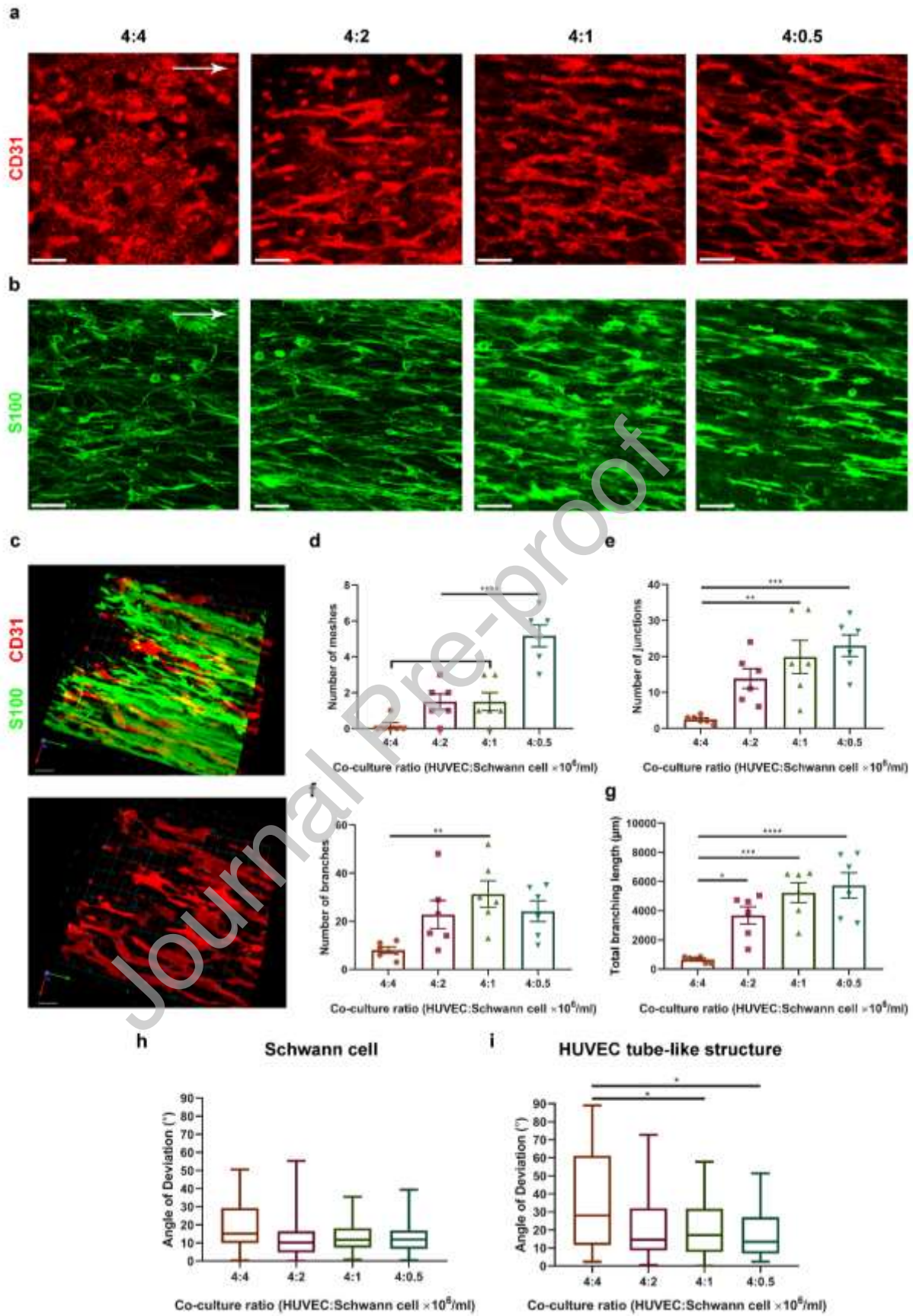
14

Figure 4. Aligned HUVEC tube-like structures in co-culture with Schwann cells in tethered collagen gels using rectangular EngNT moulds. (**a, b**) Confocal micrographs show HUVEC tube-like structures and Schwann cells aligned in co-culture at four different ratios: 4:4, 4:2, 4:1 and 4:0.5 ($\times 10^6$ cells/ml of gel). White arrow indicates longitudinal axis of the tethered gels. Scale bars, 100 μm. (**c**) Confocal 3D reconstruction illustrates tube-like vascular network and Schwann cell alignment at 4:0.5 ratio. Using ImageJ's Angiogenesis Analyser plugin, number of meshes (**d**), number of junctions (**e**), number of branches (**f**) and total branching length of the tube-like structures (**g**) was obtained and compared at the four different ratios. Data are means ± SEM. n=6 gels per condition from a total of two experimental gel batches. ****$P<0.0001$, ***$P<0.001$, **$P<0.01$, *$P<0.05$ by one-way ANOVA with Tukey's multiple comparisons test. (**h, i**) Box-and-whisker plot of Schwann cell and endothelial tube-like structure alignment, respectively (n=270 cells from 3 different experimental gel batches). The Kruskal-Wallis test was used to compute statistical significance. Scale bars, 100 μm.

3.2 HUVECs align and form tube-like structures in collagen hydrogels tethered within silicone tubes

As shown in Figure 4, aligned HUVEC tube-like structures can be produced via cellular self-alignment in tethered rectangular collagen gels. Implantation of these types of engineered tissues normally requires stabilisation to allow the gel to be removed from the tethering mould without loss of tension and structure [30-34]. However, when plastic compression was used to stabilise the aligned HUVEC gels, HUVEC viability and alignment were maintained but there was a ~50% reduction in tube-like structures (data not shown). As a result, the perforated silicone tube tethering system developed by Phillips et al. (2005) was applied in this study [29]. This system involves tethering the cellular gel within a silicone tube, using circumferential perforations at each end, enabling the tethered gel to be implanted whilst tension is maintained by the tube.

HUVECs at a density of 4×10^6 cells/ml were incorporated within the collagen hydrogels that were cast within the silicone tubes. Figure 5 shows that HUVEC gels attached to the pores created in the silicone tubes and tethered the gels to maintain tension during contraction and cellular self-alignment (Figure 5a, b). HUVECs formed tube-like structures tethered within the silicone tubes over 4 days (Figure 5c). Also, a representative confocal orthogonal projection shows lumen structures enclosed by HUVECs (Figure 5d). Formation of endothelial structures associated with angiogenesis in the silicone tube system was equivalent to the results seen in rectangular EngNT moulds (Figure 5e-5h).
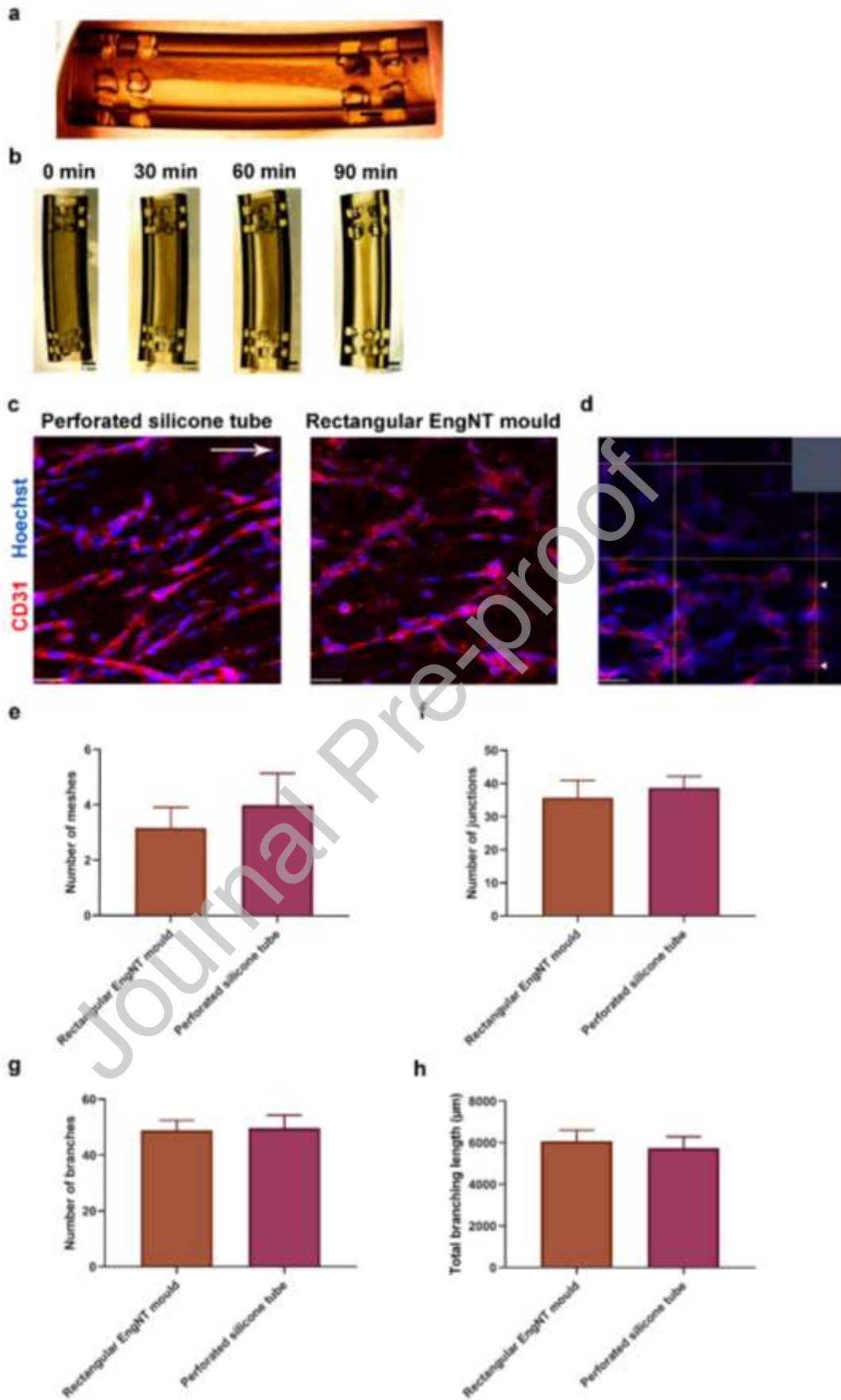
Figure 5. HUVECs aligned and formed tube-like structures in the silicone tube tethering system. HUVECs were seeded within collagen gels at 4×10^6 cells/ml which then integrated with the tethering points at the ends of the silicone tubes and allowed to contract *in vitro*. (**a**) Representative images showing a silicone tube with contracted cellular hydrogels inside at day 4 of culture. (**b**) Representative images of the hydrogel contraction in a silicone tube over 90 min at a density of 8×10^6 cells/ml. Scale bars, 1 mm. (**c**) Representative fluorescence micrographs showing HUVEC tube-like structures within the middle region of a gel tethered within a silicone tube and within a rectangular EngNT mould for 4 days of culture, immunostained for CD31. White arrow indicates longitudinal axis of the tethered gels. Scale bar, 52 μm. (**d**) Representative orthogonal view of xy confocal z slice and its respective xz (bottom) and yz (right) plane, depicting lumens of HUVEC tube-like structures (arrowheads) within a gel tethered in a silicone tube. Scale bar, 52 μm. Comparison of number of meshes (**e**), junctions (**f**), branches (**g**), and total branching length of tube-like structures (**h**) between two tethering systems: standard rectangular EngNT mould and perforated silicone tube. Data are means ± SEM. n=3 gels.

3.3 Tethered aligned HUVEC and Schwann cell constructs support nerve regeneration and vascularisation *in vivo*

A 10 mm gap rat sciatic nerve transection model was used to evaluate the potential of HUVEC-seeded aligned fully-hydrated tethered collagen constructs to promote peripheral nerve regeneration *in vivo* over 4 weeks of recovery. Six animals for each of the three groups (Schwann cell, HUVEC and HUVEC-Schwann cell) underwent surgery. Because immunocompetent wild-type rats were used, they were injected daily with cyclosporine-A to prevent immune rejection of the HUVECs. All animals received daily immunosuppression regardless of experimental group to avoid any confounding effects of the treatment. Constructs were assessed *in vivo* up to 4 weeks post-implantation, however 3/6 rats in the Schwann cell group and 3/6 rats in the HUVEC-Schwann cell group were terminated before the endpoint of the experiment due to signs of autotomy.

Repaired nerves were dissected and analysed using transverse sections through the proximal and distal end of the repair site and proximal and distal stumps (Figure 6a). All groups exhibited a similar number of axons in the proximal stumps (Figure 6b). In the proximal device, distal device and distal stump there were more axons present in the HUVEC group compared with either the Schwann cell group or the HUVEC-Schwann cell group (Figure 6b,6c).
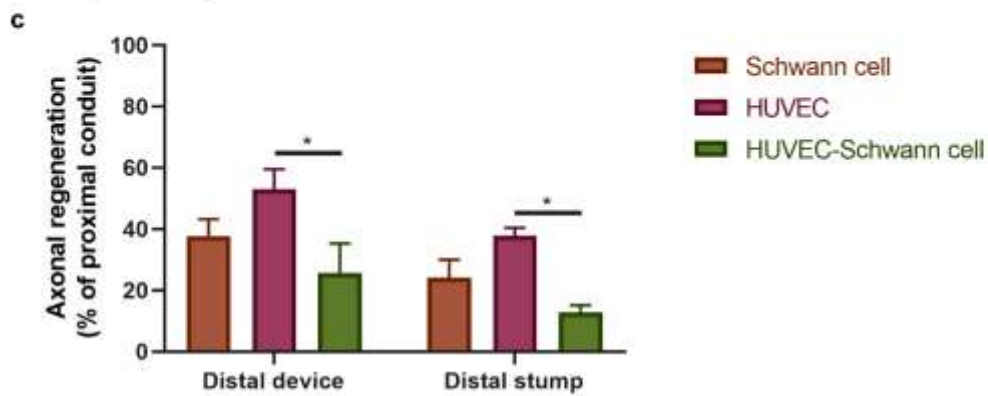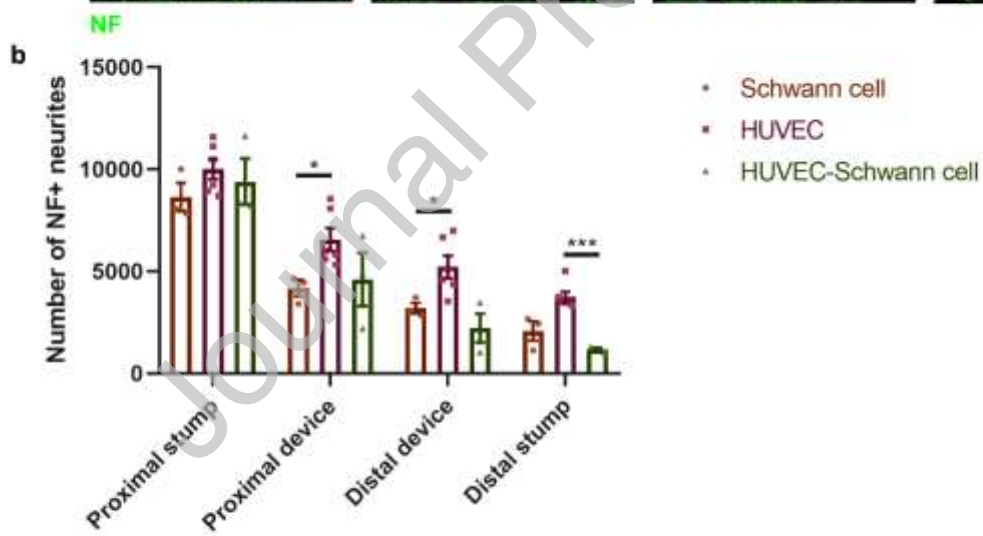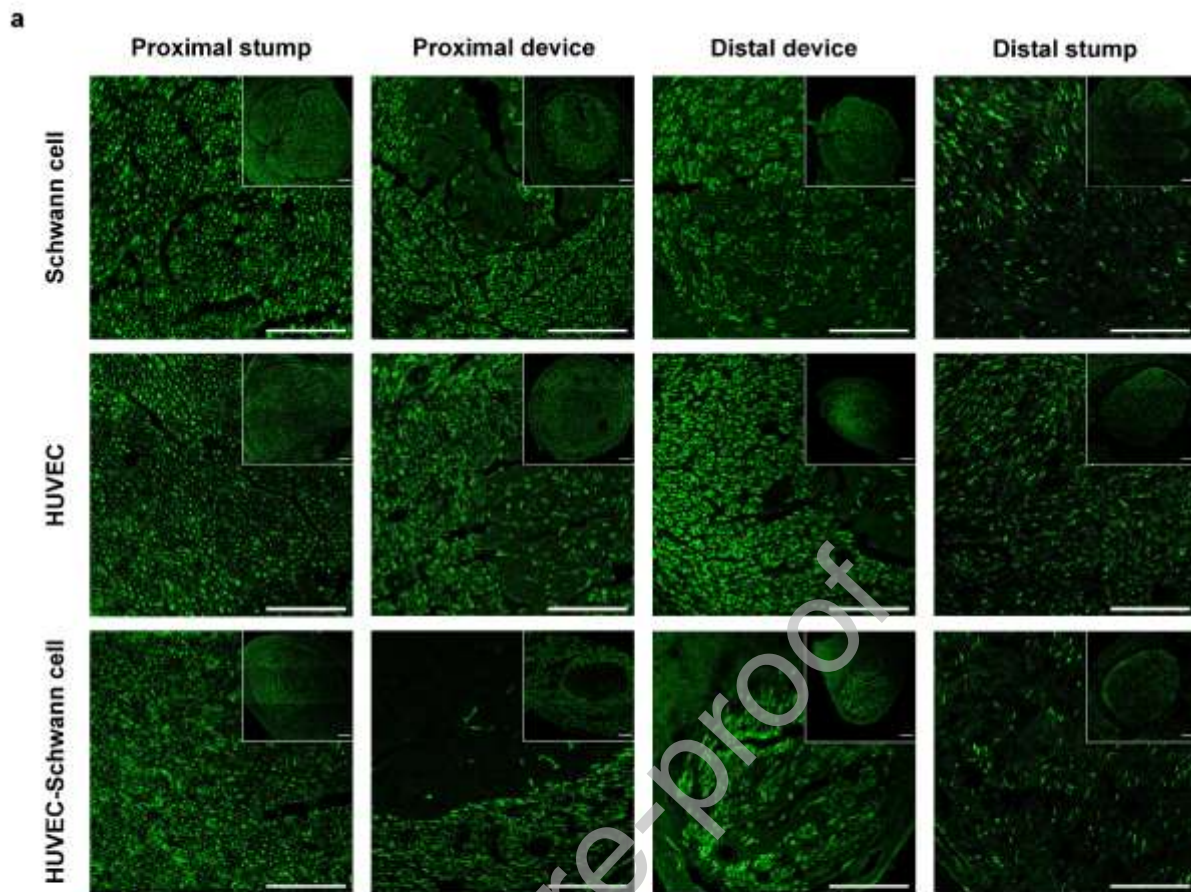
a

b

c

Figure 6. Tethered aligned HUVEC gels supported more neurite growth across a 10 mm nerve repair than gels containing Schwann cells. (**a**) Representative confocal micrographs of transverse sections showing neurofilament (NF) positive neurites at four different positions in the repaired nerves; the proximal stump, proximal device, distal device and distal stump. Scale bars, 100 μm. Insets show lower magnification views of the whole cross-sections (scale bars, 100 μm). (**b**) Quantification of the total number of neurofilament-positive axons per transverse section at the four different positions across the repair site. (**c**) Axons in the distal device and distal stump expressed as a percentage of the number of axons in the proximal part of the device in each case. Data are mean ± SEM. n=3 for Schwann cell group and HUVEC-Schwann cell group and n=6 for HUVEC group. Two-way ANOVA showed significant differences between the three treatment groups ($P<0.01$), the four sampling positions ($P<0.0001$), but no significant difference in the interaction between them. Tukey's multiple comparisons test was used to compare the three treatment groups at each sampling position and significant differences are indicated as *$P<0.05$, ***$P<0.001$.

The vascularisation of the implanted constructs was investigated via histochemical staining of transverse sections using Isolectin IB4 (detects all blood vessels, both from host rat and implanted human endothelial cells) and CD31 (specifically detects HUVECs) (Figure 7a, 7b). The majority of both CD31+ and Isolectin IB4+ blood vessels were present near the tube wall, with a few located within the collagen matrices. The HUVEC-only group showed a significantly higher number of Isolectin IB4+ blood vessels in both the proximal device and distal device region compared with the Schwann cell-containing groups (Figure 7c). Immunolabeled-CD31 showed that some transplanted HUVECs survived and formed blood vessels in both regions, although there was considerable variability in the number of CD31+ blood vessels in the distal device region with one animal in the HUVEC group showing no CD31+ blood vessels in this position (Figure 7d). There were no significant differences in the diameter of blood vessels between different locations and groups (Figure 7e).

a

	Proximal device	Distal device	Proximal device	Distal device
Schwann cell				
HUVEC				
HUVEC-Schwann cell				

Isolectin IB4   CD31

b

Number of Isolectin IB4+ blood vessels

c

Number of CD31+ blood vessels

- Schwann cell
- HUVEC
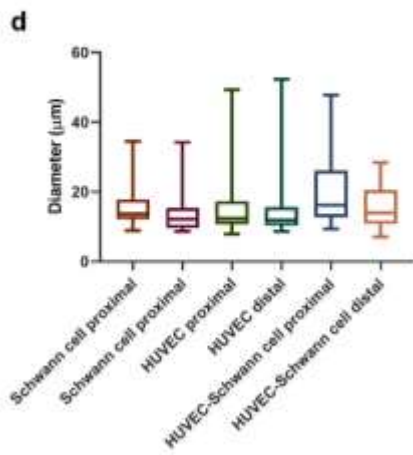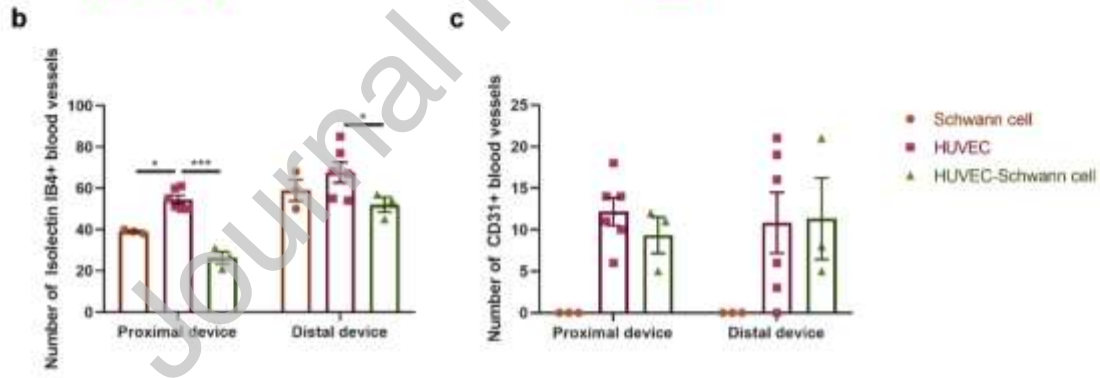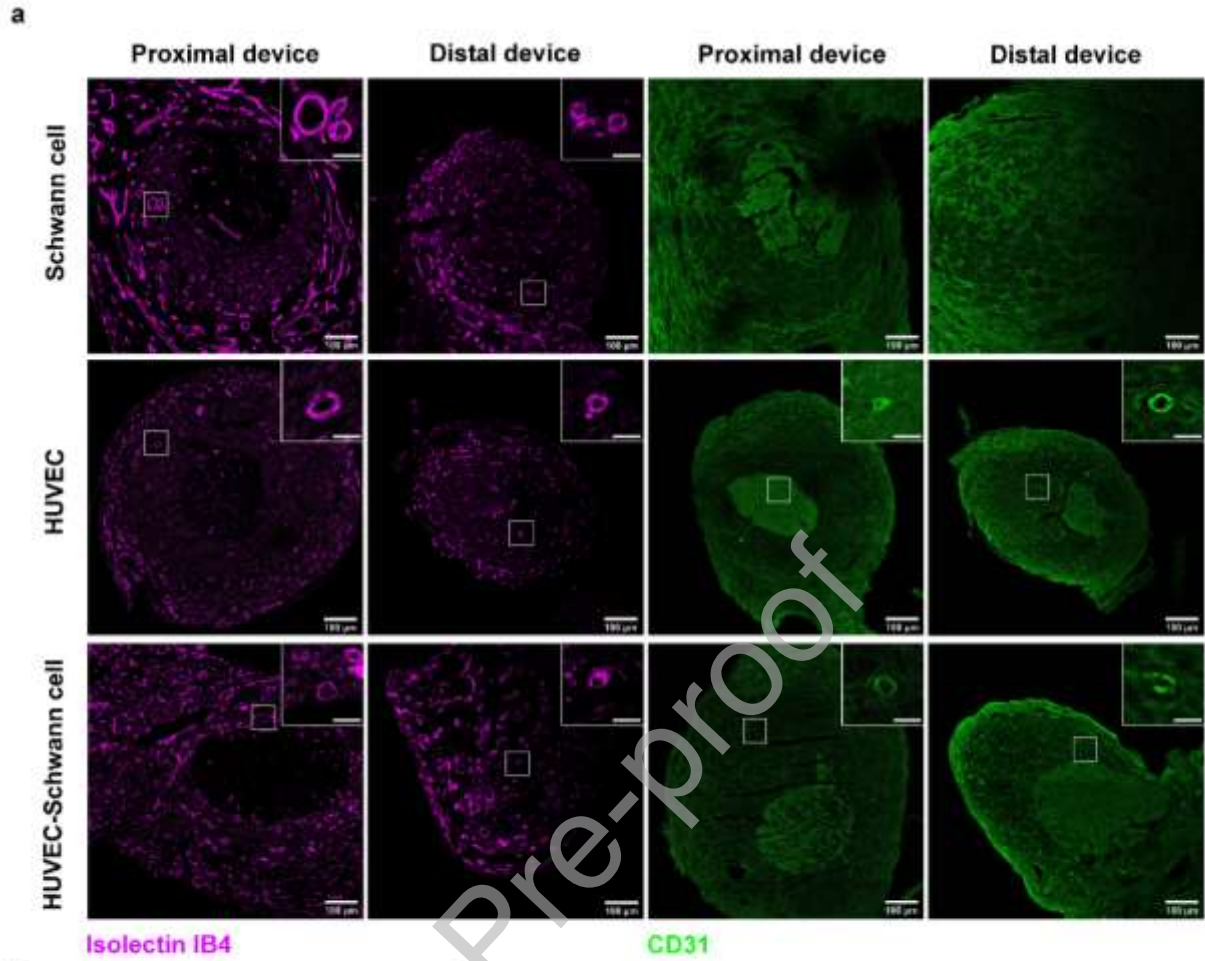- HUVEC-Schwann cell

d

Diameter (μm)

Figure 7. Vascularisation of the constructs following rat sciatic nerve repair. (**a**) Representative fluorescence micrographs of Isolectin IB4+ (detects all blood vessels, both from host rat and implanted human endothelial cells) and CD31+ (specifically detects human endothelial cells) blood vessels in transverse sections from proximal device and distal device positions, 4 weeks following repair of 10 mm rat sciatic nerve gap. Scale bars, 100 μm. Inset images show close-up lumen structures (Scale bars, 20 μm). Graphs show number of Isolectin IB4+ (**b**) and CD31+ blood vessels (**c**), and (**d**) diameter of Isolectin IB4+ blood vessels at each location. Box plots show min, max and median, with lower and upper quartile. Data are mean ± SEM. n=3 for Schwann cell group and HUVEC-Schwann cell group and n=6 for HUVEC group. Two-way ANOVA with Tukey's multiple comparisons test revealed a significant difference ($P<0.0001$) in the number of Isolectin IB4+ blood vessels and number of CD31+ (human endothelial cells) blood vessels between the proximal and distal positions analysed, and significant differences between groups, ***$P<0.001$, *$P<0.05$.

In order to determine Schwann cell migration following injury and repair, the total area of positive Schwann cell staining in transverse sections at the proximal device and distal device regions was examined in the three groups (Figure 8a). Schwann cells appeared to be mostly distributed close to the tube wall at the proximal device site and not in the collagen matrices, whereas they were more evenly distributed across the distal device site. Interestingly, there were significantly more Schwann cells present in the HUVEC group compared to the Schwann cell group at the proximal device region (Figure 8b). This trend was also present at the distal device region, however this was not significant. In contrast, there was no difference in the number of Schwann cells between the Schwann cell and HUVEC-Schwann cell group. Schwann cells were closely associated with the regenerated axons at the proximal device sites and the distal device sites in all groups (Figure 8c).
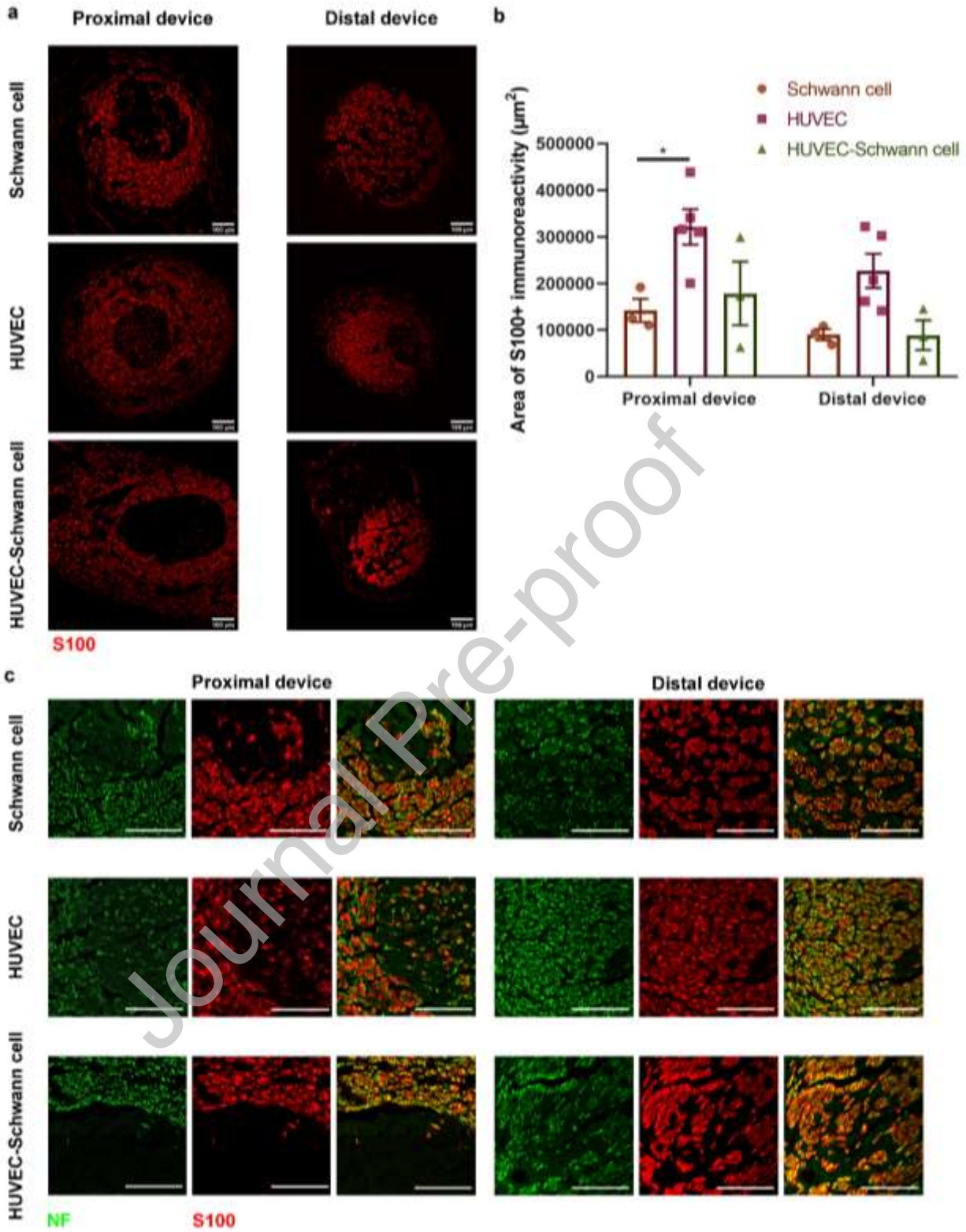
22

Figure 8. Area of Schwann cells in the constructs following rat sciatic nerve repair. (**a**) Representative fluorescence micrographs of S100+ Schwann cells in transverse sections from proximal device and distal device positions, 4 weeks following repair of a 10 mm rat sciatic nerve gap. Scale bars, 100 μm. (**b**) Area of S100+ Schwann cells at each location. Data are mean ± SEM. n=3 for Schwann cell group and HUVEC-Schwann cell group and n=6 for HUVEC group. (**c**) NF and S100 double immunohistochemistry of transverse sections from proximal device sites and distal device sites. Scale bars, 100 μm. Two-way ANOVA with Tukey's multiple comparisons test revealed a significant difference ($P<0.05$) in area of S100+ Schwann cells between the proximal and distal position, and significant differences between groups, *$P<0.05$.

4 Discussion

Vascularisation in nerve tissue engineering is important, to supply nutrients and oxygen to cellular constructs and to enhance nerve regeneration. In this study, the primary objective was to develop aligned endothelial cell structures in collagen hydrogels and to assess their efficacy in nerve repair. By using the natural ability of endothelial cells to self-align in response to cell-generated tension within tethered collagen gels, aligned 3-dimensional engineered tissues were formed. These contained highly organised tube-like human endothelial cell structures after 4 days in culture. Co-cultures of HUVECs and Schwann cells in tethered collagen gels enabled the formation of Schwann cell constructs containing microvascular network structures, providing a more sophisticated way to engineer potential nerve repair constructs that incorporate more than one cell population found in the nerve graft. This study used a tubular tethering system to deliver aligned cellular conduits into a nerve repair environment in a rat model, allowing the ability of engineered neural tissues containing aligned endothelial cell structures to support nerve regeneration to be tested *in vivo*.

HUVECs were used in this study because they are relatively easy to obtain, are robust in culture, and are capable of endothelial cell tube formation *in vitro* [38, 39]. Human endothelial cells have been shown previously to contract collagen gels [40, 41]. The optimised cell seeding density to generate aligned cells within tethered collagen constructs was identified here using a multi-well plate assay [37]. 4×10^6 HUVECs showed approximately 60% gel contraction which yielded highly aligned cells within tethered collagen gels. It has been demonstrated previously with 1.5 mg/ml collagen gels that 3×10^6 HUVECs exhibited around 65% gel contraction [41]. This is consistent with our study since cellular gels tend to contract less with higher concentrations of collagen (2 mg/ml in this case), which means more cells are needed to achieve the same contraction percentage.

The presence of aligned interconnected endothelial cell tube-like structures in collagen gels after 4 days in culture is consistent with several previous studies [25, 26, 42, 43]. In the tethered gels, after a 2-day culture period endothelial cells had started to fuse and form tubules, with the majority being individually elongated cells at this stage. Sieminski *et al.* reported that HUVECs formed elongated tube-like structures with lumens within 2 days in culture in 1.5 mg/ml constrained collagen gels [43]. Also, HUVEC-coated fibrin beads have been shown to produce sprouts at day 2 and within 5 days lumens were formed [39]. Here, tube-like structures in an 8-day gel were similar to those in 4-day gels, which is consistent with previous work that showed no great changes in network appearance, or lumen size, when endothelial cells are cultured for longer periods in collagen gels [43].

In addition to creating engineered HUVEC structures in collagen gels, the present study explored the addition of HUVEC structures to the aligned Schwann cell environment that has been used previously to support neuronal regeneration [29, 34]. Co-culture experiments *in vitro* can be challenging due to the different media requirements for individual cell populations, but in this case EGM was used because Schwann cells were shown to grow normally in this media (data not shown). Endothelial cells failed to survive and form networks when Schwann cells were present at a greater ratio than 4×10^6:1×10^6 (HUVEC:Schwann cell) in the gels. This is consistent with a previous study which demonstrated that Schwann cells can produce soluble substances, mainly TIMP-2, that inhibit angiogenesis as well as endothelial cell proliferation rate [44]. Previous work using a mouse endothelial cell line (3B-11) cultured on a matrix of basement membrane extract showed that the density of cells has a profound impact on tube formation [45]. Insufficient cells per volume yields minimal tube formation and networks, whilst at high cell density, cells appear to clump together or form monolayers. In the present study, there were few tubes and little network formation with fewer than 4×10^6 HUVECs per ml in the gels. As a result, the number of HUVECs was kept constant at 4×10^6 and the number of Schwann cells was varied, allowing different ratios to be explored and revealing that of the four options tested the ratio 4×10^6 HUVECs:0.5×10^6 Schwann cells resulted in optimal endothelial network formation and alignment.

Removal of aligned cellular gels from the tethering mould would result in loss of tension and structure. To overcome this, manufacture of EngNT using Schwann cells and various other therapeutic cell types requires stabilisation of gels using plastic compression with RAFT absorbers [30-34]. Here, it was found that RAFT stabilisation was detrimental to the integrity of the endothelial tube structures, so an alternative method for implanting the cellular gels in their tethered fully hydrated state was applied. We adapted the method developed by Phillips *et al.* (2005), where a silicone tube was perforated circumferentially near each end to create tethering sites, then used to demonstrate self-aligned Schwann cell-seeded collagen gels supported nerve regeneration across a 5 mm rat sciatic nerve injury gap at 8 weeks [29]. We found that HUVECs self-aligned and formed tube-like structures in the perforated tube tethering system after 4 days, and this was then used to deliver the cellular gels for *in vivo* tests. It should be noted that a silicone conduit was used as an outer sheath during transplantation in this study. Silicone conduits have been used extensively in animal models to investigate peripheral nerve regeneration [46-48] and also used in a 5-year follow-up clinical study by Lundborg *et al.* (2004) [49]. Silicone is not an ideal conduit material for clinical nerve repair due to its mechanical mismatch and non-biodegradability, which can cause nerve compression syndrome requiring a second operation to remove the silicone tube [50, 51]. Further studies could explore the use of degradable biomaterials that could

form a suitable outer sheath component to tether cellular gels and replace the silicone tubes for future translation to clinical application.

The rat sciatic nerve injury model was used to investigate whether a 10 mm aligned HUVEC-based engineered tissue could support nerve regeneration, and how this might compare to a construct containing Schwann cells as a more conventional approach. An additional co-culture group was included to explore the potential benefit of having both endothelial cell structures and Schwann cells present in the same material. The HUVEC constructs demonstrated a significantly greater capacity for supporting neuronal extension across the repair site when compared with the other two groups which contained Schwann cells. The HUVEC group also showed the greatest extent of vascularisation and Schwann cell infiltration, the latter being despite the additional Schwann cells delivered to the repair site in the other two groups. In this experiment it was not possible to distinguish between host and implanted Schwann cells, but based on the observations made here it would be interesting to explore the interaction between implanted and host Schwann cells in future studies. HUVECs were identifiable post-implantation through the use of human-specific CD31 antibody labelling, confirming that transplanted HUVECs survived to the 4-week end point and were present as integrated vascular structures. This corresponds to several previous studies which reported accelerated anastomosis of implanted endothelial cell-seeded hydrogel scaffolds in animal tissues [52-54]. Overall, the results of our *in vivo* study showed that engineered tissues containing aligned endothelial tube-like structures could be good candidates to treat nerve repair.

Future work could involve testing this construct in a longer gap model over a longer time, in order to establish efficacy in terms of morphometric data and functional outcomes compared with current clinical approaches (conduits and autografts). Different early time points could also be considered to examine the effect of the tissue-engineered constructs during the early stages of nerve regeneration. It would be interesting to explore why and how HUVEC tube-like structures alone outperformed similar constructs containing combinations of HUVECs and Schwann cells, since both cell types have been implicated as being beneficial in nerve repair. It is possible that the Schwann cells in the co-culture condition may have released factors that reduced the capacity of the HUVECs to form robust integrated vascular structures after implantation. Newly-formed blood vessels within the nerve bridge that forms after transection injury can serve as a scaffold to support Schwann cells adhesion and migration, resulting in enhanced axonal regeneration [7]. In this study, the HUVEC group increased Schwann cell recruitment into the nerve bridge, showing a significant difference near the proximal end of the conduit, which is consistent with the idea that vascular structures promote Schwann cell migration from nerve stumps into the repair site. It is

possible that the interaction between Schwann cells and HUVECs in the co-culture constructs, which was apparently detrimental to regeneration, vascularisation and Schwann cell migration, could be improved by decreasing the Schwann cell seeding density, the addition of exogenous angiogenic factors or the incorporation of supportive stromal cells such as fibroblasts and pericytes [52, 55, 56].

5   Conclusions

In conclusion, this study has shown that engineered tissues which contain aligned networks of endothelial cell tube-like structures can be generated in 4 days using tethered collagen gels. Engineered tissues made using HUVECs outperformed those containing Schwann cells in terms of neuronal growth, vascularisation and Schwann cell infiltration in a 10 mm rat sciatic nerve model at 4 weeks. These results highlight the dual potential of pre-vascularised engineered neural tissue constructs to provide enhanced vascularisation and direct support for regenerating axons. Future studies will need to explore the functional benefits from using nerve conduits containing aligned tube-like vascular structures to bridge longer gaps *in vivo*, over longer time points in comparison with approaches currently used in the clinic.

Declaration of interests

⊠ The authors declare that they have no known competing financial interests or personal relationships that could have appeared to influence the work reported in this paper.

Conflict of interest

The authors have no conflict of interests.

Data availability

The raw/processed data required to reproduce these findings cannot be shared at this time due to technical or time limitations.
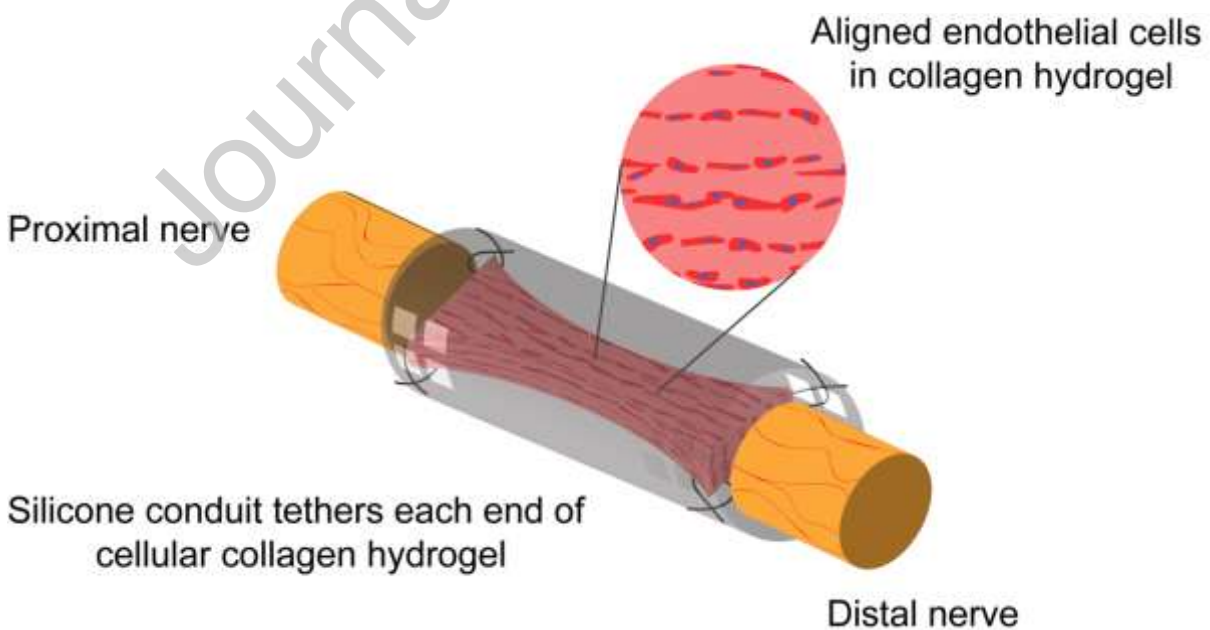
\

References

[1] E. Jabbarzadeh, T. Starnes, Y.M. Khan, T. Jiang, A.J. Wirtel, M. Deng, Q. Lv, L.S. Nair, S.B. Doty, C.T. Laurencin, Induction of angiogenesis in tissue-engineered scaffolds designed for bone repair: a combined gene therapy-cell transplantation approach, Proc Natl Acad Sci U S A 105(32) (2008) 11099-104.

[2] J. Rouwkema, J. de Boer, C.A. Van Blitterswijk, Endothelial cells assemble into a 3-dimensional prevascular network in a bone tissue engineering construct, Tissue Eng 12(9) (2006) 2685-93.

[3] D. Gholobova, L. Decroix, V. Van Muylder, L. Desender, M. Gerard, G. Carpentier, H. Vandenburgh, L. Thorrez, Endothelial Network Formation Within Human Tissue-Engineered Skeletal Muscle, Tissue engineering. Part A 21(19-20) (2015) 2548-58.

[4] A. Lesman, J. Koffler, R. Atlas, Y.J. Blinder, Z. Kam, S. Levenberg, Engineering vessel-like networks within multicellular fibrin-based constructs, Biomaterials 32(31) (2011) 7856-69.

[5] S. Levenberg, J. Rouwkema, M. Macdonald, E.S. Garfein, D.S. Kohane, D.C. Darland, R. Marini, C.A. van Blitterswijk, R.C. Mulligan, P.A. D'Amore, R. Langer, Engineering vascularized skeletal muscle tissue, Nat Biotechnol 23(7) (2005) 879-84.

[6] P. Carmeliet, M. Tessier-Lavigne, Common mechanisms of nerve and blood vessel wiring, Nature 436(7048) (2005) 193-200.

[7] A.L. Cattin, J.J. Burden, L. Van Emmenis, F.E. Mackenzie, J.J. Hoving, N. Garcia Calavia, Y. Guo, M. McLaughlin, L.H. Rosenberg, V. Quereda, D. Jamecna, I. Napoli, S. Parrinello, T. Enver, C. Ruhrberg, A.C. Lloyd, Macrophage-Induced Blood Vessels Guide Schwann Cell-Mediated Regeneration of Peripheral Nerves, Cell 162(5) (2015) 1127-39.

[8] J.M. Grasman, D.L. Kaplan, Human endothelial cells secrete neurotropic factors to direct axonal growth of peripheral nerves, Sci Rep 7(1) (2017) 4092.

[9] C. Leventhal, S. Rafii, D. Rafii, A. Shahar, S.A. Goldman, Endothelial trophic support of neuronal production and recruitment from the adult mammalian subependyma, Mol Cell Neurosci 13(6) (1999) 450-64.

[10] K. Isahara, M. Yamamoto, The interaction of vascular endothelial cells and dorsal root ganglion neurites is mediated by vitronectin and heparan sulfate proteoglycans, Brain research. Developmental brain research 84(2) (1995) 164-78.

[11] S. Jauhiainen, J.P. Laakkonen, K. Ketola, P.I. Toivanen, T. Nieminen, T. Ninchoji, A.L. Levonen, M.U. Kaikkonen, S. Yla-Herttuala, Axon Guidance-Related Factor FLRT3 Regulates VEGF-Signaling and Endothelial Cell Function, Frontiers in physiology 10 (2019) 224.

[12] S. D'Arpa, K.E.Y. Claes, F. Stillaert, B. Colebunders, S. Monstrey, P. Blondeel, Vascularized nerve "grafts": just a graft or a worthwhile procedure?, Plastic and Aesthetic Research 2(4) (2015) 183-194.

[13] T. Hasegawa, S. Nakamura, T. Manabe, Y. Mikawa, Vascularized nerve grafts for the treatment of large nerve gap after severe trauma to an upper extremity, Archives of orthopaedic and trauma surgery 124(3) (2004) 209-13.

[14] I.M. Tarlove, J.A. Epstein, Nerve grafts: the importance of an adequate blood supply, J. Neurosurg 2 (1945) 49-71.

[15] J.K. Terzis, V.K. Kostopoulos, Vascularized Nerve Grafts and Vascularized Fascia for Upper Extremity Nerve Reconstruction, Hand (New York, N.Y.) 5(1) (2010) 19-30.

[16] A. des Rieux, B. Ucakar, B.P. Mupendwa, D. Colau, O. Feron, P. Carmeliet, V. Preat, 3D systems delivering VEGF to promote angiogenesis for tissue engineering, Journal of controlled release : official journal of the Controlled Release Society 150(3) (2011) 272-8.

[17] O. Karal-Yilmaz, M. Serhatli, K. Baysal, B.M. Baysal, Preparation and in vitro characterization of vascular endothelial growth factor (VEGF)-loaded poly(D,L-lactic-co-glycolic acid) microspheres using a double emulsion/solvent evaporation technique, J Microencapsul 28(1) (2011) 46-54.

[18] G.P. Duffy, S. D'Arcy, T. Ahsan, R.M. Nerem, T. O'Brien, F. Barry, Mesenchymal stem cells overexpressing ephrin-b2 rapidly adopt an early endothelial phenotype with simultaneous reduction of osteogenic potential, Tissue engineering. Part A 16(9) (2010) 2755-68.

[19] E.G. Tierney, G.P. Duffy, A.J. Hibbitts, S.A. Cryan, F.J. O'Brien, The development of non-viral gene-activated matrices for bone regeneration using polyethyleneimine (PEI) and collagen-based scaffolds, Journal of controlled release : official journal of the Controlled Release Society 158(2) (2012) 304-11.

[20] E. Akbari, G.B. Spychalski, K.K. Rangharajan, S. Prakash, J.W. Song, Competing Fluid Forces Control Endothelial Sprouting in a 3-D Microfluidic Vessel Bifurcation Model, Micromachines (Basel) 10(7) (2019).

[21] S.J. Grainger, A.J. Putnam, Assessing the permeability of engineered capillary networks in a 3D culture, PloS one 6(7) (2011) e22086.

[22] K.T. Morin, R.T. Tranquillo, Guided sprouting from endothelial spheroids in fibrin gels aligned by magnetic fields and cell-induced gel compaction, Biomaterials 32(26) (2011) 6111-8.

[23] F. Berthod, L. Germain, N. Tremblay, F.A. Auger, Extracellular matrix deposition by fibroblasts is necessary to promote capillary-like tube formation in vitro, Journal of cellular physiology 207(2) (2006) 491-8.

[24] F. Berthod, J. Symes, N. Tremblay, J.A. Medin, F.A. Auger, Spontaneous fibroblast-derived pericyte recruitment in a human tissue-engineered angiogenesis model in vitro, Journal of cellular physiology 227(5) (2012) 2130-7.

[25] I. Montano, C. Schiestl, J. Schneider, L. Pontiggia, J. Luginbuhl, T. Biedermann, S. Bottcher-Haberzeth, E. Braziulis, M. Meuli, E. Reichmann, Formation of Human Capillaries In Vitro: The Engineering of Prevascularized Matrices, Tissue Eng Pt A 16(1) (2010) 269-282.

[26] R.L. Saunders, D.A. Hammer, Assembly of Human Umbilical Vein Endothelial Cells on Compliant Hydrogels, Cellular and molecular bioengineering 3(1) (2010) 60-67.

[27] K.T. Morin, A.O. Smith, G.E. Davis, R.T. Tranquillo, Aligned human microvessels formed in 3D fibrin gel by constraint of gel contraction, Microvascular research 90 (2013) 12-22.

[28] J.A. Schaefer, P.A. Guzman, S.B. Riemenschneider, T.J. Kamp, R.T. Tranquillo, A cardiac patch from aligned microvessel and cardiomyocyte patches, J Tissue Eng Regen Med 12(2) (2018) 546-556.

[29] J.B. Phillips, S.C. Bunting, S.M. Hall, R.A. Brown, Neural tissue engineering: a self-organizing collagen guidance conduit, Tissue Eng 11(9-10) (2005) 1611-7.

[30] C. O'Rourke, A.G.E. Day, C. Murray-Dunning, L. Thanabalasundaram, J. Cowan, L. Stevanato, N. Grace, G. Cameron, R.A.L. Drake, J. Sinden, J.B. Phillips, An allogeneic 'off the shelf' therapeutic strategy for peripheral nerve tissue engineering using clinical grade human neural stem cells, Sci Rep 8(1) (2018) 2951.

[31] M. Georgiou, J.P. Golding, A.J. Loughlin, P.J. Kingham, J.B. Phillips, Engineered neural tissue with aligned, differentiated adipose-derived stem cells promotes peripheral nerve regeneration across a critical sized defect in rat sciatic nerve, Biomaterials 37 (2015) 242-51.

[32] W. Martens, K. Sanen, M. Georgiou, T. Struys, A. Bronckaers, M. Ameloot, J. Phillips, I. Lambrichts, Human dental pulp stem cells can differentiate into Schwann cells and promote and guide neurite outgrowth in an aligned tissue-engineered collagen construct in vitro, FASEB journal : official publication of the Federation of American Societies for Experimental Biology 28(4) (2014) 1634-43.

[33] K. Sanen, W. Martens, M. Georgiou, M. Ameloot, I. Lambrichts, J. Phillips, Engineered neural tissue with Schwann cell differentiated human dental pulp stem cells: potential for peripheral nerve repair?, J Tissue Eng Regen Med 11(12) (2017) 3362-3372.

[34] M. Georgiou, S.C. Bunting, H.A. Davies, A.J. Loughlin, J.P. Golding, J.B. Phillips, Engineered neural tissue for peripheral nerve repair, Biomaterials 34(30) (2013) 7335-43.

[35] K. Sanen, R. Paesen, S. Luyck, J. Phillips, I. Lambrichts, W. Martens, M. Ameloot, Label-free mapping of microstructural organisation in self-aligning cellular collagen hydrogels using image correlation spectroscopy, Acta Biomater 30 (2016) 258-264.

[36] C.A. Schneider, W.S. Rasband, K.W. Eliceiri, NIH Image to ImageJ: 25 years of image analysis, Nature Methods 9(7) (2012) 671-675.

[37] C. O'Rourke, R.A. Drake, G.W. Cameron, A. Jane Loughlin, J.B. Phillips, Optimising contraction and alignment of cellular collagen hydrogels to achieve reliable and consistent engineered anisotropic tissue, Journal of biomaterials applications 30(5) (2015) 599-607.

[38] I. Arnaoutova, J. George, H.K. Kleinman, G. Benton, The endothelial cell tube formation assay on basement membrane turns 20: state of the science and the art, Angiogenesis 12(3) (2009) 267-74.

[39] M.N. Nakatsu, R.C.A. Sainson, J.N. Aoto, K.L. Taylor, M. Aitkenhead, S. Pérez-del-Pulgar, P.M. Carpenter, C.C.W. Hughes, Angiogenic sprouting and capillary lumen formation modeled by human umbilical vein endothelial cells (HUVEC) in fibrin gels: the role of fibroblasts and Angiopoietin-1☆, Microvascular research 66(2) (2003) 102-112.

[40] X.D. Liu, M. Skold, T. Umino, Y.K. Zhu, D.J. Romberger, J.R. Spurzem, S.I. Rennard, Endothelial cell-mediated type I collagen gel contraction is regulated by hemin, The Journal of laboratory and clinical medicine 136(2) (2000) 100-9.

[41] M.D. Stevenson, A.L. Sieminski, C.M. McLeod, F.J. Byfield, V.H. Barocas, Keith J. Gooch, Pericellular Conditions Regulate Extent of Cell-Mediated Compaction of Collagen Gels, Biophysical Journal 99(1) (2010) 19-28.

[42] A.M. Schor, I. Ellis, S.L. Schor, Collagen gel assay for angiogenesis : induction of endothelial cell sprouting, Methods in molecular medicine 46 (2001) 145-62.

[43] A.L. Sieminski, R.P. Hebbel, K.J. Gooch, The relative magnitudes of endothelial force generation and matrix stiffness modulate capillary morphogenesis in vitro, Experimental cell research 297(2) (2004) 574-84.

[44] D. Huang, J.L. Rutkowski, G.M. Brodeur, P.M. Chou, J.L. Kwiatkowski, A. Babbo, S.L. Cohn, Schwann cell-conditioned medium inhibits angiogenesis, Cancer research 60(21) (2000) 5966-71.

[45] K.L. DeCicco-Skinner, G.H. Henry, C. Cataisson, T. Tabib, J.C. Gwilliam, N.J. Watson, E.M. Bullwinkle, L. Falkenburg, R.C. O'Neill, A. Morin, J.S. Wiest, Endothelial Cell Tube Formation Assay for the In Vitro Study of Angiogenesis, Journal of visualized experiments : JoVE (91) (2014).

[46] S.M. Kim, S.K. Lee, J.H. Lee, Peripheral nerve regeneration using a three dimensionally cultured schwann cell conduit, J Craniofac Surg 18(3) (2007) 475-88.

[47] F. Wu, D. Xing, Z. Peng, T. Rao, Enhanced rat sciatic nerve regeneration through silicon tubes implanted with valproic acid, Journal of reconstructive microsurgery 24(4) (2008) 267-76.

[48] L.J. Chamberlain, I.V. Yannas, A. Arrizabalaga, H.P. Hsu, T.V. Norregaard, M. Spector, Early peripheral nerve healing in collagen and silicone tube implants: myofibroblasts and the cellular response, Biomaterials 19(15) (1998) 1393-403.

[49] G. Lundborg, B. Rosen, L. Dahlin, J. Holmberg, I. Rosen, Tubular repair of the median or ulnar nerve in the human forearm: a 5-year follow-up, J Hand Surg Br 29(2) (2004) 100-7.

[50] F. Stang, G. Keilhoff, H. Fansa, Biocompatibility of Different Nerve Tubes, Materials (Basel) 2(4) (2009) 1480-1507.

[51] A. Muheremu, Q. Ao, Past, Present, and Future of Nerve Conduits in the Treatment of Peripheral Nerve Injury, Biomed Res Int 2015 (2015) 237507.

[52] X. Chen, A.S. Aledia, S.A. Popson, L. Him, C.C. Hughes, S.C. George, Rapid anastomosis of endothelial progenitor cell-derived vessels with host vasculature is promoted by a high density of cotransplanted fibroblasts, Tissue engineering. Part A 16(2) (2010) 585-94.

[53] S. Ben-Shaul, S. Landau, U. Merdler, S. Levenberg, Mature vessel networks in engineered tissue promote graft-host anastomosis and prevent graft thrombosis, Proc Natl Acad Sci U S A 116(8) (2019) 2955-2960.

[54] G. Cheng, S. Liao, H. Kit Wong, D.A. Lacorre, E. di Tomaso, P. Au, D. Fukumura, R.K. Jain, L.L. Munn, Engineered blood vessel networks connect to host vasculature via wrapping-and-tapping anastomosis, Blood 118(17) (2011) 4740-9.

[55] Y. Wang, D. Li, G. Wang, L. Chen, J. Chen, Z. Liu, Z. Zhang, H. Shen, Y. Jin, Z. Shen, The effect of co-transplantation of nerve fibroblasts and Schwann cells on peripheral nerve repair, Int J Biol Sci 13(12) (2017) 1507-1519.

[56] F. Laredo, J. Plebanski, A. Tedeschi, Pericytes: Problems and Promises for CNS Repair, Front Cell Neurosci 13 (2019) 546.

Graphical abstract